Feasibility Study of Online Monitoring Using the Fiber Bragg Grating Sensor for Geared System

Shenghao Shi
School of Mechanical and Electronic Engineering
Wuhan University of Technology
Wuhan, P.R. China
shenghao_shi910@163.com

Yongzhi Qu
School of Mechanical and Electronic Engineering
Wuhan University of Technology
Wuhan, P.R. China
quwong@whut.edu.cn

Jinglin Wang
Aviation Key Laboratory of Science and Technology on Fault Diagnosis and Health Management
Shanghai, P.R. China
scenelin@163.com

Liu Hong
School of Mechanical and Electronic Engineering
Wuhan University of Technology
Wuhan, P.R. China
hongliu@whut.edu.cn

Jaspreet Singh Dhupia
School of Mechanical Engineering
University of Auckland
20 Symonds St, City Center 1010 New Zealand
j.dhupia@auckland.ac.nz

Zude Zhou
School of Mechanical and Electronic Engineering
Wuhan University of Technology
Wuhan, P.R. China
Zudezhou@whut.edu.cn

***Abstract*—The gearbox is one of the most common and important components in the drivetrains. Thus, the online monitoring of the dynamic behavior of geared system is crucial for the optimization, diagnosis and prognosis of the drivetrains. The conventional online monitoring system for gearboxes is to use the vibration sensor mounted on the gear housing. However, in the measured housing vibration signal, the dynamic response of the monitored geared pair is usually distorted, which is caused by the complex transfer path of the vibration. Therefore, to advance the art of online monitoring of gearboxes, this work proposes to employ the fiber Bragg grating as the strain sensor to mount near the gear mesh region. The experimental assessment of the feasibility of the fiber Bragg grating based online monitoring system is conducted in a laboratory fixed-axis spur gearbox. To validate and analyze the measurement from the fiber Bragg grating system, a gear mesh model is developed using the finite element method. The comparison between the measurement and theoretical simulation show the proposed fiber Bragg grating based online monitoring system is capable to capture the variation of the root strain during the gear mesh process. This result proves the proposed technique has a promising potential in developing a commercial online monitoring system to measure the subtle dynamic behavior of gearboxes.**

Keywords; FBG sensors;dynamic strain; finite element model

I. INTRODUCTION

The gearbox has been widely applied in industrials because it is one of most vital components in the drivetrains. The efficiency and safe operation of the gearbox directly decide the performance and reliability of the whole drivetrains. Thus, the condition monitoring of gearboxes is significantly important, which can improve the safety and reduce the maintenance cost of the whole system. The vibration based monitoring techniques have been widely studied and used for the online monitoring of gearboxes, in which the vibration sensor is mounted on the gear housing to measure the dynamics response of the gear mesh process. The measured housing vibration signal has been proven that it contains rich information about the health state of the gearbox. Previous studies have also studied gearbox vibrations and explained the effects of vibration on gear operation [1-4]. However, in certain cases, such monitoring system may fail to detect the gear fault or give false alarm, which is usually due to the signal distortion of the transfer path from the gear mesh region to the gear housing. To address such issue, the resistance strain gage can be pasted near the gear mesh region to directly measure the dynamic response of geared pair. Although the resistance strain gage shows its success in monitoring of the gear mesh process in laboratory, the large-scale use of the resistance strain gage for gearboxes is stilled limited in industrials because of its complex wiring problem of cables.

In the recent, with the characteristics such as light weight, small size, electromagnetic interference immunity and long-distance transmission, the fiber Bragg grating (FBG) based sensors have attracted the interest of many researchers [5-10]. After engraving the Bragg reflector in a short segment of an optical fiber, the segment, called as FBG, reflects a particular wavelength of light and transmits all the others. Moreover, the reflected wavelength of light by FBG is shifted with the change of temperature or strain of the segment. Thus, the FBG can be used as the temperature or strain sensor. The FBG sensors have an inherent serial multiplexing capacity. It means that the multiple FBGs can be serially engraved on one fiber, which

The work is supported by National Natural Science Foundation of China (Grant No.51605349) and Aeronautical Science Foundation of China (Grant No.20173365001)

978-1-7281-0860-5/19/$31.00 ©2019 IEEE

forms a large capacity sensing network without the messy wiring problem.

To advance the state of art of the online monitoring of geared system, this study investigates the feasibility of FBG based strain sensor for the online monitoring of geared system. In the experiment, the FBG was pasted on the end face of a tested spur gear, which is near the gear mesh region to measure the dynamic strain excited by the gear mesh process. Although there are a few existing literature reporting the possibility of diagnosis of gears using FBG of the measured features haven't been explained and analyzed in details. To assess the measured feature and validate the measurement by the FBG containing rich information of the gear mesh process, this work develops a quasi-static gear mesh model in ANSYS. The comparison between the experimental measurement and theoretical simulation show the proposed FBG based online monitoring system is capable to capture the subtle behavior during the gear mesh process.

The rest of the paper is organized as follows: Section 2 gives a brief review on the sensing principle of FBG and the detailed setup of the experimental test rig is introduced. The key steps of building the transient gear mesh model in ANSYS are described in Section 3. Section 4 compares the simulated root strain of a spur gear from the ANSYS and the experimental measurement from the FBG sensor. Finally, Section 5 concludes the paper.

II. Setup of The Experimental Test Rig

The sensing principle of FBG sensors is briefly reviewed at the beginning of this section. Then, the detailed setup of a spur gearbox test rig instrumented with the FBG sensor is introduced in the later part of this section.

A. Sensing Principle of The FBG

The FBG is the Bragg reflector can be engraved to a short segment of the optical fiber by exposing under a periodic pattern of ultraviolet light. The length of the exposed short segment is usually chosen to be around 5mm to 10mm, which is called as FBG. Based on the principle of Bragg reflection, the FBG works similar to a spectral reflector: when a broadband incident light illuminates into a fiber and meets with a FBG, a particular wavelength of light will be reflected back and the rest of light continues to transmit through the fiber. Such particular wavelength is defined as the Bragg wavelength λ. This phenomenon is illustrated in Fig. 1. The Bragg wavelength λ can be expressed as:

$$\lambda=2n_{eff}\Lambda \tag{1}$$

where n_{eff} and Λ are the refractive index of the core material determined by the material properties of the optical fiber itself and the grating period adjustable by the exposing periodic pattern of ultraviolet light, respectively. When the temperature and axial strain of a FBG changes, it is found that the Bragg wavelength λ is also shifted due to the variation of n_{eff} and Λ. Such Bragg wavelength shift of FBG, $\Delta\lambda$, caused by the change of the axial strain $\Delta\varepsilon$ and temperature ΔT, can be written as:

$$\frac{\Delta\lambda}{\lambda}=\left(1-\rho_e\right)\cdot\Delta\varepsilon+\left(\alpha_f+\xi\right)\cdot\Delta T \tag{2}$$

where λ is the initial central wavelength of FBG. ρ_e, α_f and ξ are the effective photo-elastic coefficient, the thermal expansion coefficient and the thermal-optic coefficient of fused silica fiber, respectively. Those coefficients can be treated as constant under the normal temperature condition. Moreover, as the temperature is usually a slow variety, after the decline or high pass filtering, wavelength shift contributed from the varying temperature can be eliminated. Thus, though the FBG is cross-sensitive with the temperature and strain, the FBG have the potential to be used as a strain sensor to measure dynamic strain response in the rotary machine.

With the multiplexing technologies like the wavelength division multiplexing, the FBG based sensors are easily to form a large capacity sensing network that is free of the messy wiring problem. Fig. 2 illustrates such FBG sensing network using just one fiber, in which multiple FBG with different initial Bragg wavelength are engraved in this optical fiber. Note that this work only focus on the examination of the performance of a single FBG for online monitoring of gear mesh, the performance of the FBG sensing network for gearboxes will be examined in the near future.

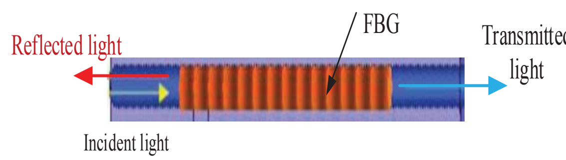

Figure 1. The working principle of FBG.

With the multiplexing technologies such as wavelength division multiplexing, time division multiplexing and spatial division multiplexing, the FBG sensors are able to form a large capacity sensing network where multiple Bragg gratings are engraved in one optical fiber as illustrated in Fig. 2.

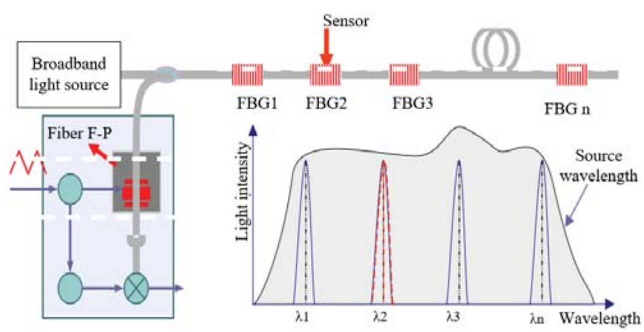

Figure 2. A FBG network with the wavelength division multiplexing.

As shown in Fig. 3, a single stage of fixed-axis spur gearbox was used as the test rig. The gear ratio of the spur gearbox was 1.8 where the driving pinion has 40 gear teeth and the driven wheel has 72 gear teeth. The detailed system parameters of the spur gear pair are summarized in TABLE I.

The gearbox was driven by a 45kW Siemens permanent magnetic motor and another permanent magnetic motor was used as the generator in this test rig to provide the load to the gearbox. In this test rig, the generated electrical power was recycled to the driving end to improve the power efficiency.

B. Gearbox Test Rig Employing the FBG Based Strain Sensor

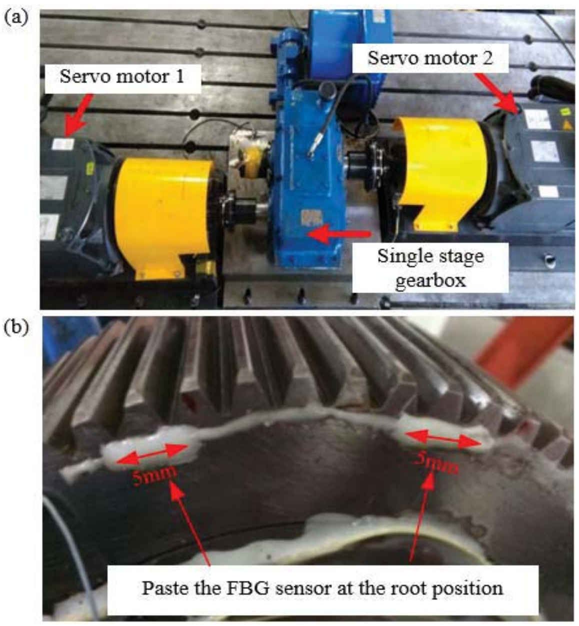

Figure 3. (a) The spur gearbox; (b) employed FBGs.

TABLE I. The parameters of the spur gear

Parameters	Pinion	gear
Number of teeth	40	72
Module(mm)	3	3
Young's module(pa)	2.0×10^{11}	2.0×10^{11}
Poisson's ratio	0.3	0.3
Tooth width(mm)	85	85
Pressure angle(°)	20	20
Pitch diameter(mm)	120	216
Base circle diameter(mm)	112.763	202.974
Center distance(mm)	168	168
The addendum coefficient	1	1
The tip clearance coefficient	0.25	0.25

Due to the very limited addendum clearance (only 0.75 mm) in the tested spur gear pair, it was difficult to directly mount the FBG inside the addendum clearance. Consequently, as illustrated in Fig. 4(b), two 5mm FBGs were pasted on the end face of the driven wheel as the strain sensor. A method of measuring the root strain at a similar position is also reported in the paper [11-12]. The mounted locations were chosen along the based circle because the locations were still near to the gear mesh region and assumed to be sensitive to the dynamic strain contributed from the gear mesh. The shaft of the driven wheel was manufactured as hollow so that the routing of the optical fiber was able to go through the shaft and embed inside the gearbox. As shown in Fig. 4(a), the end of the optical fiber, rotating with the shaft, was connected to the stationary interrogator by employing the fiber optic rotary joint. The sampling frequency of the interrogator was set as 5000Hz (fs = 5000Hz) in this experiment, which was used to monitor the Bragg wavelength shift of the FBGs.

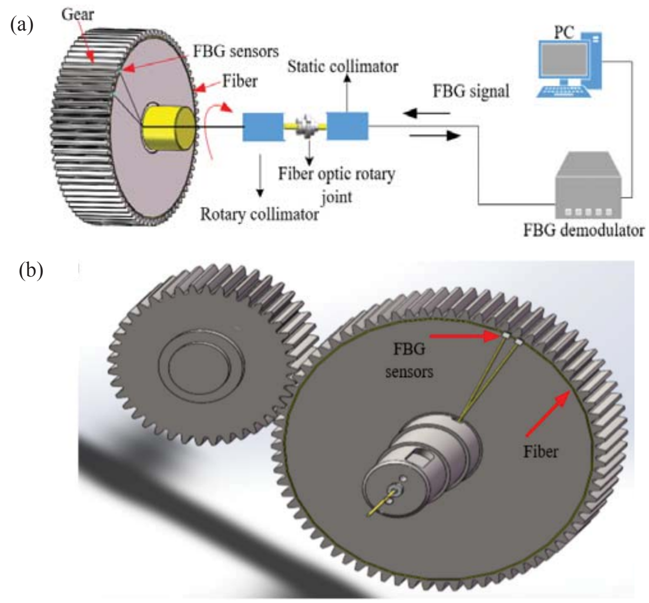

Figure 4. (a) Schematic of the test rig; (b) the mounted locations of FBG sensors.

III. GEAR MESH MODEL BASED ON THE FINITE ELEMENT APPROACH

The finite element analysis consists four main steps. A gear model is built in ANSYS Workbench to simulate the response of the root strain during the gear mesh process, which is compared with the experimental measurement to assess the performance of the proposed FBG based online monitoring system. First, the three dimensional geometric model of the gear pair is created and assembled in SOLIDWORKS based on the system parameters listed in TABLE I. Because the main concern of the simulation is to investigate the response of the root strain, the radius of the hub hole is intentionally increased as shown in Fig. 5 to reduce the complexity of the model in ANSYS that has very little influence on the simulated root strain [13]. Then, the assembled 3D gear pair model in SOLIDWORKS can be imported into ANSYS Workbench without losing any design details. For the ease of readers, the key steps to conduct the simulation in ANSYS Workbench are describe as follows. Gearbox test rig employing the FBG based strain sensor.

A. Setting of Material Properties of the Gear Pair

The properties of the structural material must be set before the importation of the SOLIDWORKS model. In order to have a more realistic solution, the material of the gear body is chosen as the structural steel in ANSYS Workbench and the other setting of the detailed material properties are given in Fig.6 for the interest of readers.

B. Setting of the Contact of Gear Teeth

The properties of the contact of gear teeth are needed to set after the importation of the 3D gear pair model. The specific settings used in this simulation. The contact between the gear and pinion teeth is defined as frictional and the coefficient of friction is chosen as 0.1 in this study. At the same time, the gear contact normal stiffness is set to be 3. The formulation is chosen as "Augmented Lagrange" and the interface treatment is set as

Adjust to Touch that makes the numerical solution easier to converge and accelerate the computation process [14].

C. Mesh of the 3D Gear Model and Analysis Settings

As the hexahedral mesh is efficient for the deformation analysis where the strain gradient changes greatly, the imported gear model is meshed with the hexahedral element SOLID185. The contact element types of the driving pinion and driven wheel are chosen as contact 174 and target 170. Fig. 7(a) shows the meshed model in this study that contains a total of 343176 nodes and 70560 elements. The transient analysis module of ANSYS is chosen to analyze the response of root strain during the gear mesh process. The related settings are given in Fig. 7(b). ANSYS workbench has different setting systems for different situations. For this study, the Transient Structure is set for quasi-static analysis.

D. Definition of Boundary Conditions and Post-Process

The hubs of the driving pinion and driven wheel are connected with "body-ground revolute joint" that assumes the gears only retain the rotational degree of freedom. In order to mimic the realistic rotational process of the gear pair, an angular velocity is applied to the driving pinion and a torque is applied to the driven wheel as shown in Fig.8 (a). A probe as given in Fig. 8(b) is used to extract the value of root strain during the simulated gear mesh process.

Figure 5. 3D model built in SOLIDWORKS.

	A	B	C	D	E
1	Contents of Engineering Data			Source	Description
2	Material				
3	Structural Steel			G	Fatigue Data at zero mean stress comes from 1998 ASME BPV Code, Section 8, Div 2, Table 5-110.1

Properties of Outline Row 3: Structural Steel

	A	B	C	D	E
1	Property	Value	Unit		
2	Material Field Variables	Table			
3	Density	7850	kg m^-3		
4	Isotropic Secant Coefficient of Thermal Expansion				
6	Isotropic Elasticity				
7	Derive from	Young's M...			
8	Young's Modulus	2E+11	Pa		
9	Poisson's Ratio	0.3			
10	Bulk Modulus	1.6667E+11	Pa		
11	Shear Modulus	7.6923E+10	Pa		
12	Alternating Stress Mean Stress	Tabular			
16	Strain-Life Parameters				
24	Tensile Yield Strength	2.5E+08	Pa		
25	Compressive Yield Strength	2.5E+08	Pa		
26	Tensile Ultimate Strength	4.6E+08	Pa		
27	Compressive Ultimate Strength	0	Pa		

Figure 6. Setting of the material properties in Engineering Date.

(a)

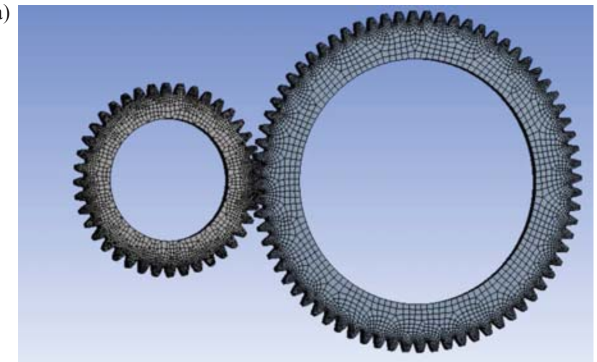

(b)

Details of "Analysis Settings"

Step Controls	
Number Of Steps	1.
Current Step Number	1.
Step End Time	1. s
Auto Time Stepping	On
Define By	Substeps
Initial Substeps	50.
Minimum Substeps	20.
Maximum Substeps	1000.
Time Integration	On
Solver Controls	
Solver Type	Program Controlled
Weak Springs	Program Controlled
Large Deflection	On
Restart Controls	
Nonlinear Controls	
Output Controls	
Damping Controls	
Stiffness Coefficient...	Direct Input
Stiffness Coeffici...	0.
Mass Coefficient	0.
Numerical Damping	Program Controlled
Numerical Damping...	0.1
Analysis Data Management	
Visibility	

Figure 7. (a) The mesh model of the gear pair;(b) analysis settings for simulations.

(a)

(b)

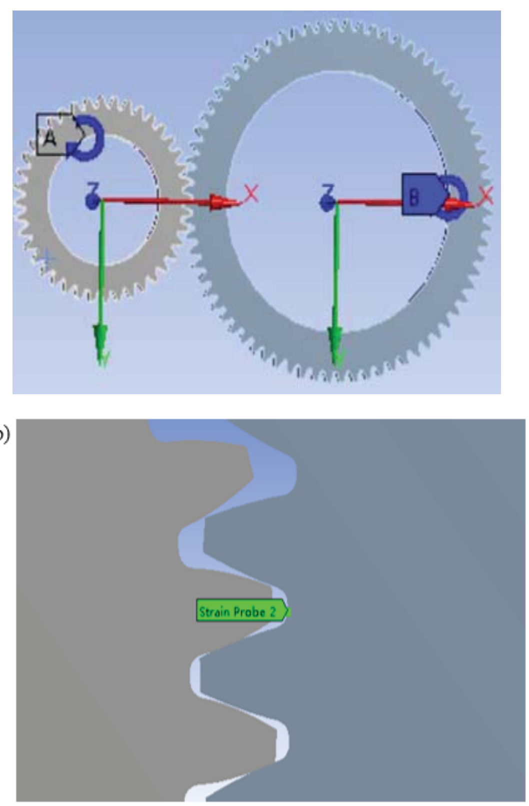

Figure 8. (a) The load applied on the gear hub ;(b) a probe used to extract root strain.

IV. Discussion on the Simulated and Experimental Result

A. Gear Root Strain for Healthy Tooth

The measured root strain from the experimental test rig and the simulated root strain from the developed finite element model are shown in Fig. 9. It can be observed that the trend of the measurement and the simulated dynamics matches well, which proves the capability of FBG based sensor in the application of online monitoring of gearboxes. In the experiment, the spur gearbox was operated under the speed 500RPM and 300Nm torque was applied as the load. In Fig. 9(a), the double tooth contact zone are marked as I and III, while the single tooth contact zone is marked as II. Thus, it can be observed that the duration of the total mesh period of a single tooth in the experiment was around 11.2ms. On the other hand, in the simulated case, to speed up the convergence of the solver, a quasi-static case was simulated, in which the applied speed and torque to the driving pinion and driven wheel was set as 62RPM and 300Nm, respectively. The duration of overall mesh circle for a single tooth in the simulated case was around 89ms as shown in Fig. 9(b). During the simulated study, the maximum value of the root strain was found to happen at the end of the single tooth contact zone and the minimum vale of the root strain (a negative value) was found at the end of the double tooth contact zone as illustrated in Fig. 10. This phenomenon is further explained by Fig. 11 where the mesh force in the single tooth contact zone introduces a tension effect to a certain point in the tooth root and then the mesh force in the double tooth contact zone gives a compression effect to that point [15]. The simulated and experimental result in this section proves the proposed FBG based online monitoring system can capture the subtle dynamic root strain behavior during the gear mesh process.

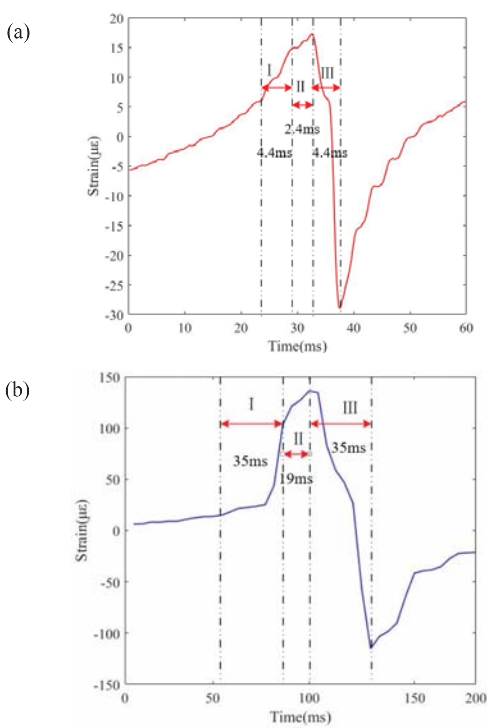

Figure 9. (a) Root strain measurement with FBG; (b) root strain from FEM.

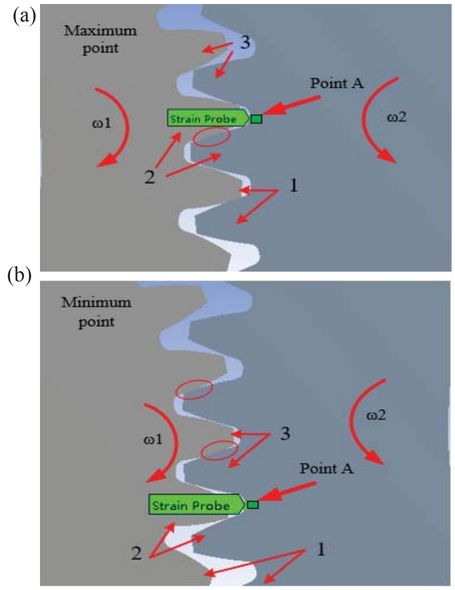

Figure 10. (a) The gear mesh condition when point A having the maximum root strain;(b) the gear mesh condition when point A having the minimum root strain.

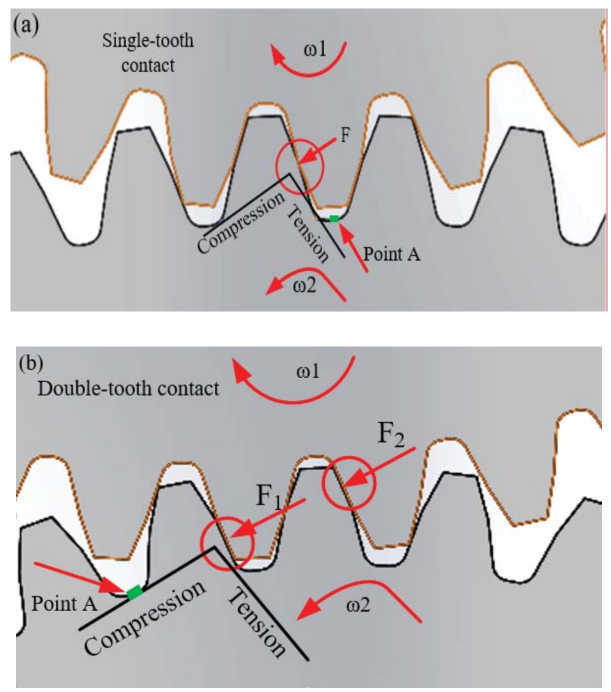

Figure 11. (a) The tensile effect for point A ;(b) the compressed effect for point A.

B. Gear Root Strain for Cracked Tooth

A simulated study was also conducted to explore the behavior of gear tooth strain for cracked tooth. The studied geometric parameters of the crack are shown in Fig.12, where *q*, *v* and *ψ* represent, the crack depth, the crack propagation direction and the crack initiation position, respectively. Assuming that the crack penetrates all along the tooth width direction, and the crack propagation angle was set as 45° and the crack depth was set as 2 mm in the simulation. The element type of the cracked tooth was still meshed with the hexahedral in the

ANSYS. The simulated gear root strain of a cracked tooth (red line) is compared with the gear root strain of a healthy tooth (blue line) in Fig. 13. It can be observed that the cracked tooth results a drop in the root strain. As such drop can be measured by the proposed FBG sensing technique, the proposed monitoring system in this paper has potential to be used to develop an online diagnostic system for gearboxes.

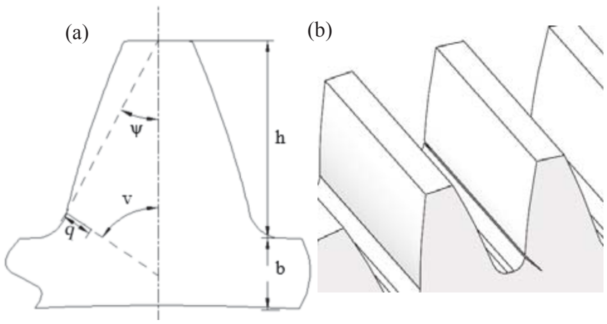

Figure 12. (a)The geometric parameters of the crack;(b) the 3D model of crack.

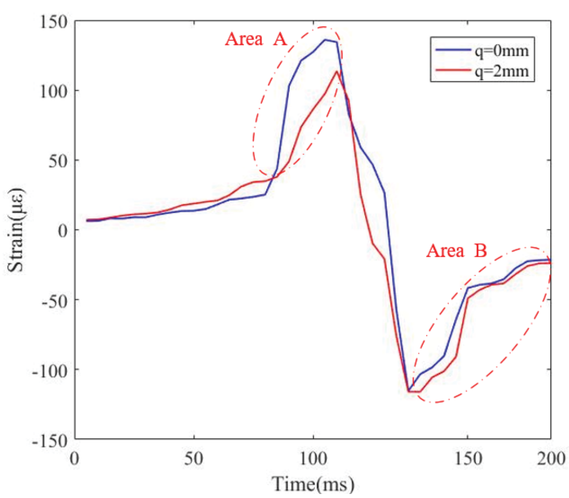

Figure 13. Simulated root strain for cracked tooth from FEM.

V. CONCLUSION

This work proposes to employ FBG as the strain sensor for the online monitoring of gearboxes, which is easy to embed inside the gearbox to approach the gear mesh region and does not interfere with the normal operation of the gearbox. The experiment was conducted on a single stage spur gearbox, in which the FBGs were mounted along the base circle of the gear body due to the limited addendum clearance. The optical signal was transmitted through the fiber optic rotary joint from the rotating end to the stationary end. A 5 kHz interrogator was used to demodulate the Bragg wavelength shift of the FBG. On the other hand, a finite element model is developed in ANSYS to study the characteristics of root strain during the gear mesh process. It is found that the measurement from the FBG based sensor matches well with the simulated dynamics of root strain of the gear tooth, which proves the FBG based sensor is capable to capture the subtle dynamic behavior of gearboxes. Therefore, the FBG based sensing network has a promising potential to be used to develop an economic and reliable online monitoring system for gearboxes in industrials.

ACKNOWLEDGMENT

This research is supported by National Natural Science Foundation of China (Grant No. 51605349) and Aeronautical Science Foundation of China (Grant No. 20173365001).

REFERENCES

[1] S. Jia, I. Howard, and J. Wang, “The Dynamic Modeling of Multiple Pairs of Spur Gears in Mesh, Including Friction and Geometrical Errors,” Int. J. Rotating. Mach, vol. 9, pp. 437-442, November 2003.

[2] W. Bartelmus, “Mathematical Modelling and Computer Simulations as an Aid to Gearbox Diagnostics,”Mech. Syst. Signal. Pr, vol. 15, Issue 5, pp. 855-871, September 2001.

[3] T. Eritenel, and R. G. Parker, “Three-dimensional nonlinear vibration of gear pairs,"J. Sound. Vib, vol. 331, Issue 15, pp.3628-3648, July 2012.

[4] I. Howard, S. Jia, and J. Wang, “The Dynamic Modelling of a Spur Gear in Mesh Including Friction and a Crack,”Mech. Syst. Signal. Pr, vol 15, pp. 831-853, September 2001.

[5] H. Guo, G. Xiao, N. Mrad, and J. Yao, “Fiber Optic Sensors for Structural Health Monitoring of Air Platforms,” Sensors-Basel, vol. 11, pp. 3687-3705, December 2011.

[6] J. S. Kiddy, P. D. Samuel, D. G. Lewicki, K. E. LaBerge, R. T. Ehinger, and J. Fetty, “Fiber optic strain sensor for planetary gear diagnostics,” NASA Glenn Res. Center, Cleveland, OH, USA, Technical Report NASA/TM-2011-217123, November 2011.[67th Annual Forum and Technology Display, United States,2011].

[7] C. S. Baldwin, J. S. Kiddy, and P. D. Samuel, “Towards development of a fiber optic-based transmission monitoring system,” in Proc. Spie, Alex A. Kazemi, Bernard Kress, Eric Y. Chan, Nabeel A. Riza and Lothar U. Kempenvol, Eds, vol. 8026N, pp. 19-20, May 2011.

[8] D. Chen, L.S. Huo, H. Li, and G.B. Song, “A Fiber Bragg Grating (FBG)-Enabled Smart Washer for Bolt Pre-Load Measurement: Design, Analysis, Calibration, and Experimental Validation,” Sensors-basel, vol. 18, Issue 8, August 2018.

[9] J. Huang, C.Q. Ji, Z.C. Wang and Z.D. Zhou, “Multi-parameter dynamical measuring system using fiber Bragg grating sensors for industrial hydraulic piping,” Measurement, vol. 134, pp. 226-235, October 2019.

[10] Q. Zhao et al, “Novel integrated optical fiber sensor for temperature, pressure and flow measurement,” Sensors. Actuat. A-Phys, vol. 280, pp. 68-75, July 2018.

[11] N. K. Raghuwanshi, and A. Parey, “Experimental Measurement of Gear Mesh Stiffness of Cracked Spur Gear by Strain Gauge Technique,” Measurement, vol 86, pp. 266-275, May 2016.

[12] S. S. Patil, S. Karuppanan, and I. Atanasovska, “Experimental measurement of strain and stress state at the contacting helical gear pairs,” Measurement, vol. 82, pp. 313-322, March 2016.

[13] Miryam B. Sánchez , Miguel Pleguezuelos and José I. Pedrero, “Approximate equations for the meshing stiffness and the load sharing ratio of spur gears including hertzian effects,”Mech. Mech. Theory, vol. 109, pp.231-249, March 2017.

[14] J. Zhang, “A-CAD-FEM-QSA integration technique for determining time-varying meshing stiffness of gear pairs,” Mesurement, vol. 100, pp. 139-149, March 2017.

[15] B. A. Shotter, “A new approach to gear tooth root stress,” J. Eng. Ind, vol. 96, pp. 11-18, February 1974.